Article

Solid State Gas Sensors with Ni-based Sensing Materials for Highly Selective Detecting NOx

ZhengHu Zhang , ChengHan Yi , Tao Chen , YangBo Zhao , YanYu Zhang , Han Jin *

Posted Date: 23 October 2024

doi: 10.20944/preprints202410.1837.v1

Keywords: NOx gas sensor; Yttria-stabilized zirconia (YSZ); High selectivity; Inhaled nitric oxide; Ni-based sensing materials

Article

Solid State Gas Sensors with Ni-Based Sensing Materials for Highly Selective Detecting NOx

ZhengHu Zhang [1,†], ChengHan Yi [1,†], Tao Chen [2], Yangbo Zhao [2], Yanyu Zhang [2] and Han Jin [1,3,4,5,*]

[1] Institute of Micro-Nano Science and Technology & National Key Laboratory of Advanced Micro and Nano Manufacture Technology, School of Electronic Information and Electrical Engineering, Shanghai Jiao Tong University, Shanghai 200240, P. R. China
[2] Nanjing Novlead Biotechnology Co. Ltd, Nanjing 211800, P. R. China
[3] Medical School, Henan University, Kaifeng 475004, Henan Province, P. R. China
[4] National Engineering Research Center for Nanotechnology, Shanghai 200241, P. R. China
[5] Wuzhen Laboratory, Tongxiang 314500, Zhejiang Province, P. R. China
* Correspondence: jinhan10@sjtu.edu.cn
† These authors contributed equally.

Abstract: Precise monitoring of NO_x concentrations in nitric oxide delivery systems is crucial to ensure the safety and well-being of patients undergoing inhaled nitric oxide (iNO) therapy for pulmonary arterial hypertension. Currently, NO_x sensing in commercialized iNO instruments predominantly relies on chemiluminescence sensors, which not only drives up costs but also limits their portability. Herein, we developed solid state gas sensors utilizing Ni-based sensing materials for effectively tracking the level of NO and NO_2 in NO delivery system. These sensors comprised of NiO-SE or ($NiFe_2O_4$+30 wt.% Fe_2O_3)-SE vs. Mn-based RE demonstrated high selectivity towards 100 ppm NO under the interference of 10 ppm NO_2 or 3 ppm NO_2 under the interference of 100 ppm NO, respectively. Meanwhile, excellent stability, repeatability, and humidity resistance were also verified for proposed sensors. Sensing mechanisms were thoroughly investigated through assessments of adsorption capabilities and electrochemical reactivity. It turns out that the superior electrochemical reactivity of NiO towards NO, alongside with the NO_2 favorable adsorption characteristics of ($NiFe_2O_4$ + 30 wt.% Fe_2O_3), is the primary reason for the high selectivity to NO_x. These findings indicate a bright future for the application of these NO_x sensors in innovative iNO treatment technologies.

Keywords: NOx gas sensor; yttria-stabilized zirconia (YSZ); high selectivity; inhaled nitric oxide; Ni-based sensing materials

1. Introduction

Pulmonary arterial hypertension (PAH) is a complex and fatal emergency of vascular disorder which affects more than 100 million people worldwide, and mainly found in neonates [1,2]. Compared with oral medicine or injection, inhaled nitric oxide (iNO), a pulmonary vasodilator approved by the Food and Drug Administration (FDA), offers several advantages in the PAH treatment such as noninvasive, targeted fast onset of action and less severe systemic adverse effect [3–5]. This method, depending on the severity of disease, usually involves the continuous administration of NO gas in the range of 100 ppm by nasal plug or mask [6,7]. However, during treatment the concentration of NO delivered needs to be tightly controlled in the first place, otherwise it may cause a rebound in pulmonary arterial pressure and endanger the patient's life [8]. Additionally, a certain amount of low concentration NO_2 may be generated during the transport of NO, which also should be precisely detected timely because such a toxic gas can directly endanger patient's health when the concentration is above 3 ppm [9,10].

It's worth noting that commercialized iNO systems generally using chemiluminescence devices to measure NO and NO_2, which limits the portability and leads to very high cost [3,11]. In recent years, with the rapid development of gas sensors, NOx gas sensors based on solid state YSZ (yttria-

 doi:10.20944/preprints202410.1837.v1

stabilized zirconia)-based electrolyte have received extensive attention from researchers due to their high selectivity, desirable sensitivity and satisfactory stability [12–18]. Besides, YSZ-based sensors can be fabricated in planar configuration, greatly simplifying the structure of the sensor and facilitating the development of integration for commercially available products [13,19,20]. However, currently reported mixed-potential NOx gas sensors mainly focus on the detection of NO and NO_2 in the middle-to-high concentration range of 100-500 ppm in automotive and industrial contexts [21–25], while the iNO treatment instrument normally requires relatively low NOx detection limit. What's more, it's a great challenge to selectively detect 3 ppm NO_2 with 100 ppm NO interference, tens of times the difference in concentration. Herein, we proposed high performance YSZ-based NOx sensors by screening out optimal sensing materials. Sensing characteristics of the developed sensors were systematically studied. Besides, adsorption capabilities and electrochemical reactivity of these sensors were characteristics to clarified the working principle

2. Experimental

2.1. Fabrication of Sensors

Figure 1 depicted the schematic components of the planar sensor. Initially, commercial MnO_2 powder (99% purity, Sigma-Aldrich Chemie GmbH, Taufkirchen, Germany) was thoroughly mixed with α-terpineol and the obtained paste was painted on the YSZ plate (length × width × thickness: 2.75 × 0.5 × 0.1 cm^3; NIKKATO CORPORATION, Osaka, Japan) , after drying at 130°C for 4h, the YSZ plate attached with the MnO_2 layer was calcined at 1400°C for 2h in a muffle furnace to form the Mn-based reference electrode (RE). Various commercial metal oxides (Sigma Aldrich Chemie GmbH, with a purity of 99%) were fabricated with the similar procedure and both calcined at high temperature for 2h to form the sensing electrodes (SE).

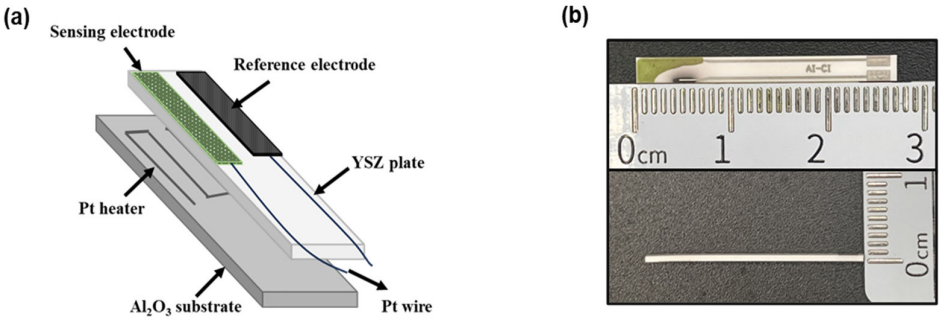

Figure 1. (a) Schematic illustration of the planar YSZ-based gas sensor; (b) the fabricated miniaturized YSZ-based sensor.

2.2. Evaluation of Sensing Characteristics

The fabricated sensor was set in a quartz tube, and alternatively exposed to the base gas (21 vol.% O_2, N_2 balance) or the sample gas containing NO, NO_2 (total flow rate: 100 mL·min-1) for 5 minutes. The NO tested concentration range was 10-100 ppm in 21 vol% O_2, N_2 balance and the NO_2 tested concentration range was 1.5-10 ppm in 21 vol% O_2, N_2 balance. An adjustable DC power supply (SS-3305D, A-BF, China) controls the Pt heater's working voltage to provide a high working temperature for the sensors. The electrochemical signals were recorded by a Data Acquisition/Switch Unit (34970A, Agilent, China) via Pt wire connected and the potential difference ΔV ($\Delta V = V_{\text{Sample gas}} - V_{\text{Base gas}}$) represented the sensor's response to sample gas. The surface morphology of calcined powders was observed by Atomic Force Scanning Electron Microscope (Gemini 360, Carl Zeiss, Germany) with an excitation voltage of 15 kV and the crystalline phase was characterized by X-ray diffraction (D8 DaVinci, Bruker, Germany). Finally, microcantilever chips and an integrated Gas Sensing System (LoC-GSS 1000, High-End MEMS Technology, China) were utilized to test the sensing materials' gas adsorption.

 doi:10.20944/preprints202410.1837.v1

3. Results and Discussion

3.1. Screening of Nitric Oxide Sensing Materials and Developing High Performance NO Sensor

Several metal oxides were selected as potential candidate for NO sensing material and among the examined SEs, In_2O_3-SE gave not only the highest potential value to 100 ppm NO but also higher potential value to 10 ppm NO_2, resulting in poor NO selectivity (Figure 2). In contrast, NiO-SE showed both desirable NO sensitivity and selectivity in compared with other examined materials. Consequently, NiO was pretended to be the optimal materials for NO detection due to the higher sensitivity and selectivity.

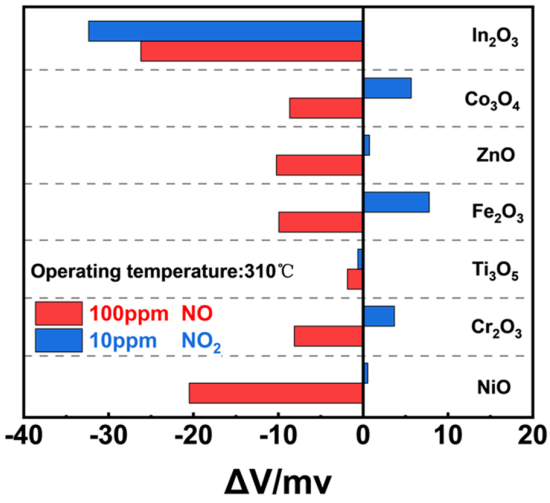

Figure 2. Comparison of sensing responses to 100 ppm NO and 10 ppm NO_2 in air.

The SEM image in Figure 3 showed that the NiO powder annealed at 1200°C were plate-like and relatively compact. According to former research that plate-like metal oxides normally exhibited better selectivity to NO [26,27], we anticipated desirable selectivity for NiO towards NO when against NO_2.

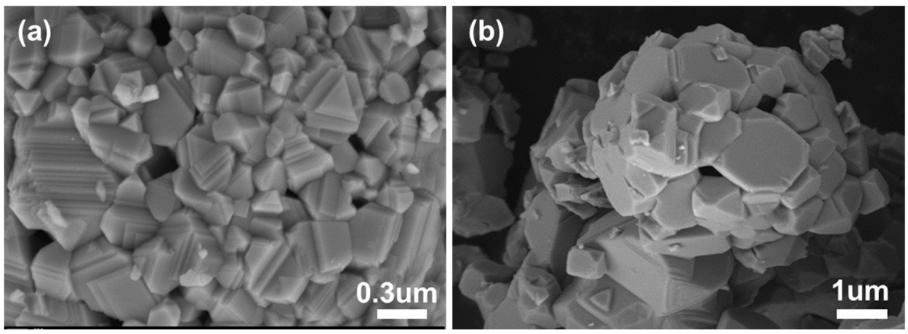

Figure 3. SEM image of NiO powder calcined at 1200°C in different scale.

To confirm the practicability of using NiO tracking high level of NO with high selectivity against 10 ppm NO_2, sensing characteristics of the YSZ-based gas sensor comprised of NiO-SE vs. Mn-based RE was studied. Figure 4(a) depicted the relationship between sensor's response and the operating/calcination temperature for the NiO-SE, it can be confirmed that optimal response signal was observed for the sensor fabricated at 1200°C and operated at 310°C. Consequently, the optimal operating/calcination temperature was selected at 310°C and 1200°C for the following study. As shown in Figure 4(b), response signal of the sensor varied linearly to the logarithm of the NO concentration in the range of 10-100 ppm. According to the repeated response transients of the sensor that exposed to 100 ppm NO and 10 ppm NO_2 (Figure4(c)), it can be concluded that the sensor gave

 doi:10.20944/preprints202410.1837.v1

excellent repeatability in the successive runs and high selectivity to 100 ppm NO (24.7 mV) against 10 ppm NO_2 (less than 1 mV). In light of the long-term stability is crucial factor in practical applications. A 35-days test to 100 ppm NO was further measured under 310°C, as shown in Figure 4(d), variation of the response value during the tested period was roughly estimated to be less than 3 mV, indicating satisfactory stability of the sensor using NiO-SE and Mn-based RE.

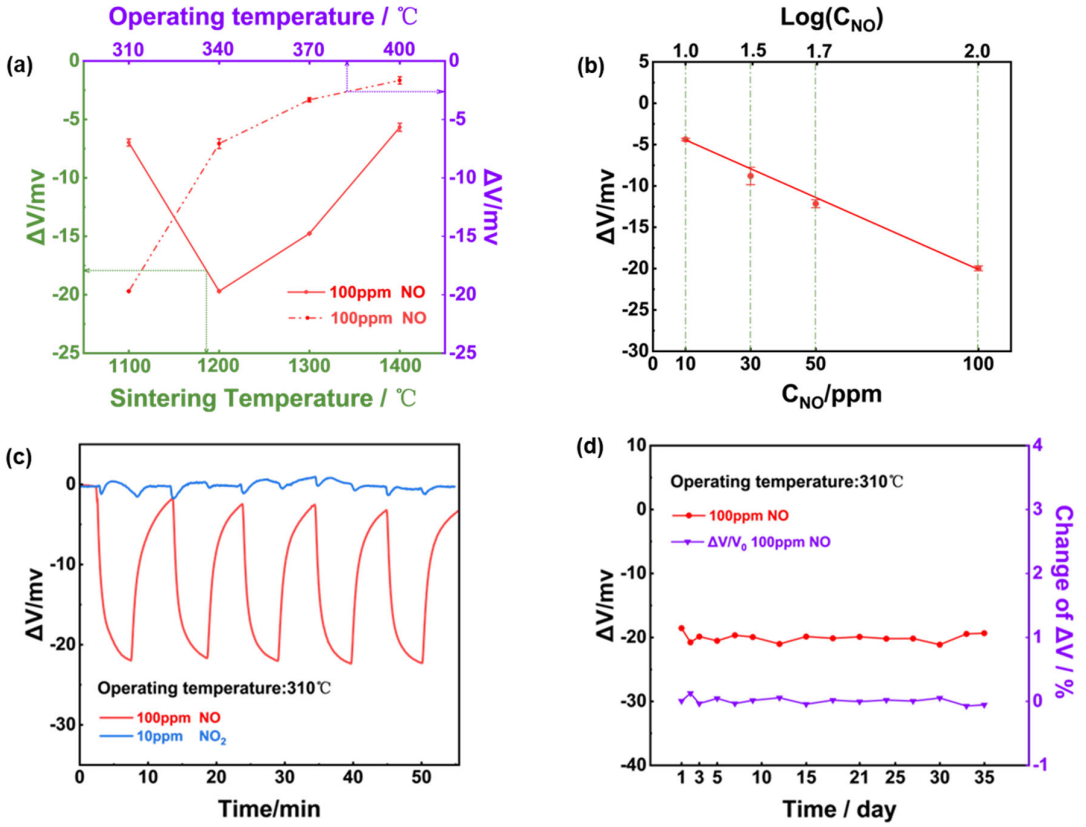

Figure 4. Sensing characteristics of the NiO-SE NO sensor in 21% O_2 with N_2 balance. (a) variation of the response signal to 100 ppm NO on the operational/calcination temperature; (b) dependence of the response signal on the logarithm of the NO concentration in the range of 10-100 ppm at 310°C; (c) repeated response transients to 100 ppm NO and 10 ppm NO_2 of the sensor at at 310°C; (d) long-term stability of the sensor to 100 ppm NO within 35-days.

3.2. Screening of Nitric Dioxide Sensing Materials and Developing High Performance NO_2 Sensor

It's a great challenge to detect low concentration of NO_2 compared to tenth times concentration of NO, and pure metal oxides as sensing materials are hardly to realize the research target. Recently, spinel-based oxides have been proved to be good candidates for NO_x sensing. For instance, $NiFe_2O_4$ was reported to be a potential NO_2 sensing material but the inadequate detection limit (LOD) down to 5 ppm limits its application in iNO treatment technologies [23,28,29]. In order to improve the sensing behavior to NO_2, it is believed that adding additives or dopants to $NiFe_2O_4$ would effectively extend the LOD [30,31]. In the meantime, Fe_2O_3 was announced that not only exhibited the same trivalent cation as the $NiFe_2O_4$'s AB_2O_4 general formula but also demonstrated acceptable capability to detect NO_2 [32]. Thus, we added Fe_2O_3 into $NiFe_2O_4$ in an attempt to enhance the NO_2 detection capacity.

Figure 5 demonstrated the XRD patterns for $NiFe_2O_4$, Fe_2O_3 and ($NiFe_2O_4$+x wt.% Fe_2O_3) composites after calcined at 1200°C for 2h. It is confirmed that the prepared composites at the different ratio of Fe_2O_3 were found to be highly crystalline without impurity, as all the XRD peak can be indexed to the pure $NiFe_2O_4$, Fe_2O_3 without the formation of new phase.

 doi:10.20944/preprints202410.1837.v1

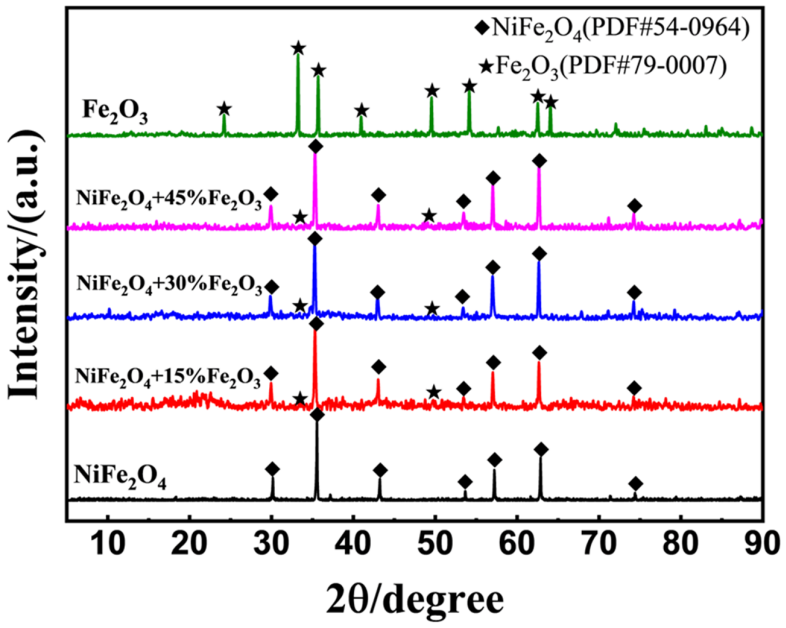

Figure 5. XRD patterns of $NiFe_2O_4$, Fe_2O_3 and ($NiFe_2O_4$+x wt.% Fe_2O_3) composites (x=15%, 30%, 45%), with calcined at 1200°C for 2h.

Furthermore, micro-structure of $NiFe_2O_4$, Fe_2O_3 and their composite (e.g. $NiFe_2O_4$+30 wt.% Fe_2O_3) were characterized via scanning electron microscope (SEM) and presented in Figure 6. In comparison with $NiFe_2O_4$ (Figure6(a), (b)) and Fe_2O_3 (Figure6(c), (d)), a certain amount of grains (with the diameter of around 0.6 μm) which could be assigned to $NiFe_2O_4$ were observed in the $NiFe_2O_4$+30 wt.% Fe_2O_3 composite. Besides, it is reasonable to deduce that the formed composite owned more porous and three-dimensional (3D) structure when compared with that of $NiFe_2O_4$. The porous 3D micro-structure would offered more active reaction sites for NO_2.

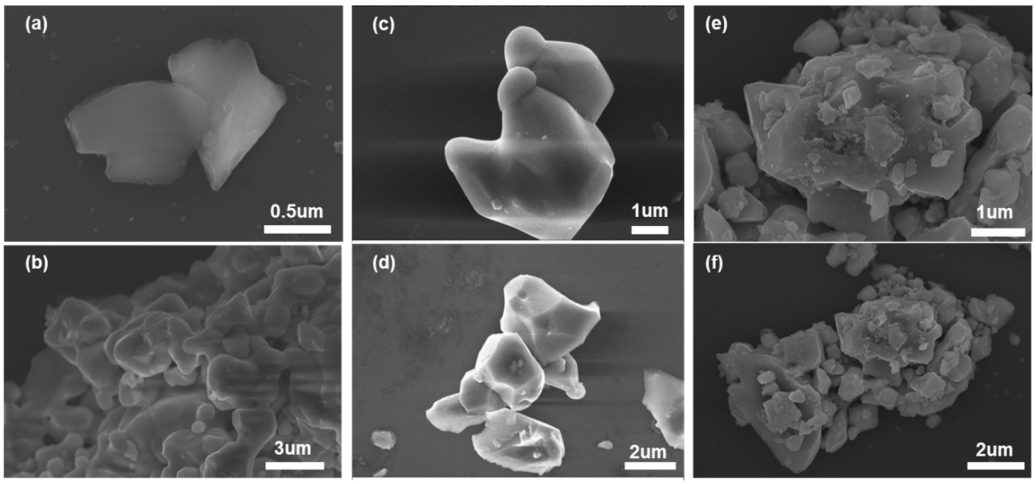

Figure 6. SEM images of (a), (b) $NiFe_2O_4$; (c), (d) Fe_2O_3; (e), (f) $NiFe_2O_4$+30 wt.% Fe_2O_3 composite sensing electrode prepared at 1200°C in different scale.

Accordingly, sensing behavior to detect 3 ppm NO_2 and 100 ppm NO for the YSZ-based gas sensor utilizing $NiFe_2O_4$ and its composite-SEs (vs. Mn-based RE) was examined. As shown in Figure 7(a), when the amount of of Fe_2O_3 reaches 30%, the sensor gave superior selectivity and sensitivity to 3 ppm NO_2 against 100 ppm NO. In other words, the YSZ-based gas sensor using ($NiFe_2O_4$+30 wt.%

 doi:10.20944/preprints202410.1837.v1

Fe_2O_3)-SE is a good candidate to tracking the trace amount of NO_2. Figure 7(b) suggested the optimal operating/calcination temperature was 390°C/1200°C.

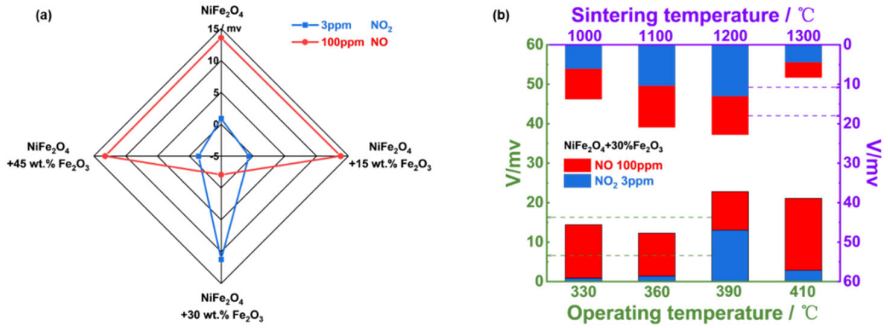

Figure 7. (a) Response magnitude to 3 ppm NO_2 and 100 ppm NO in 21% O_2 with N_2 balance respectively for the YSZ-based sensors comprising $NiFe_2O_4/Fe_2O_3$ composite SEs and Mn-based RE, operated at 390°C; (b) effect of change in operating/sintering temperature on the sensing characteristic of the sensor using ($NiFe_2O_4$+30 wt.% Fe_2O_3)-SE in 21% O_2 with N_2 balance.

The dependence of the sensing response on the NO_2 concentration in the range of 1.5-10 ppm was examined and a linear relationship between response value and NO_2 concentration on a logarithmic scale (Figure 8(a)). Notably, it can be concluded that after aging for several days (2-3 days), response signal of the sensor to 100 ppm NO significantly decreased whereas maintained a high response value to 3 ppm NO_2 (Figure 8(b)). Figure 8(c, d) further indicated the sensor's excellent repeatability and stability as well as ultra-high selectivity to 3 ppm NO_2.

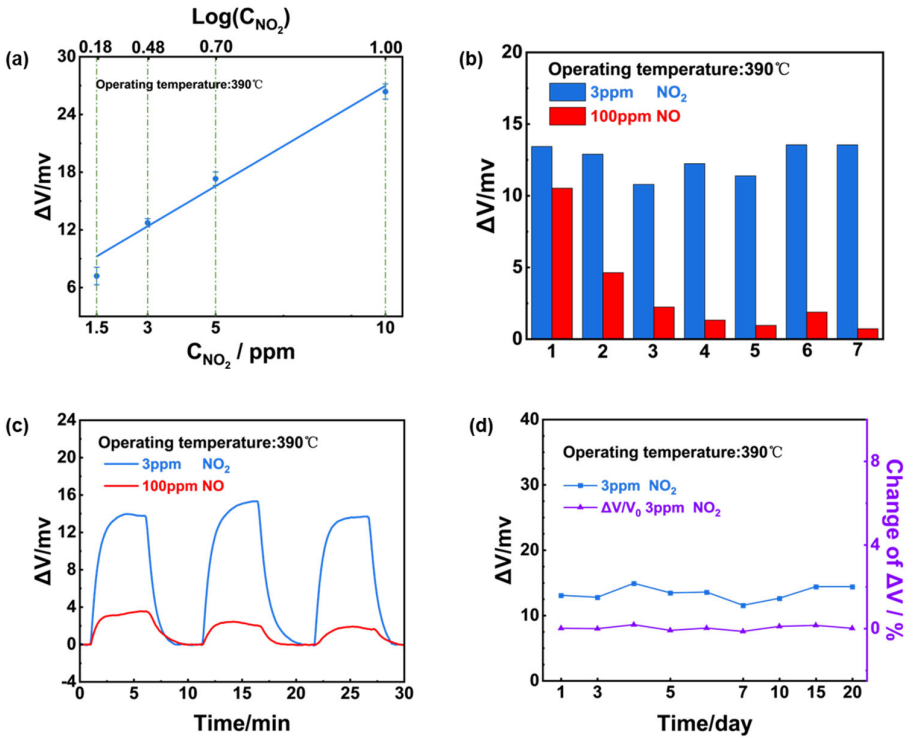

Figure 8. Sensing characteristics of the YSZ-based gas sensor using ($NiFe_2O_4$+30 wt.% Fe_2O_3)-SE. (a) Dependence of the response signal on the logarithm of the NO_2 concentration in the range of 1.5-10 ppm at 390°C; (b) repeated response to 3 ppm NO_2 and 100 ppm NO during aging process; (c) repeated response transients to 3 ppm NO_2 and 100 ppm NO; (d) long-term stability of the sensor to 3 ppm NO_2 within 20-days.

 doi:10.20944/preprints202410.1837.v1

3.3. Study on the Sensing Mechanism

According to the working principle of electrochemical gas sensor, target gas initially selective adsorbs on the surface of the sensing material and then participates the followed electrochemical reaction. In this case, both adsorption capabilities and electrochemical reactivity contribute the final response selectivity and response value. To understand which step primary determine the widely concerned selectivity during NO_x sensing, we initially used microgravimetric technology [33,34] to comparing the NO_x adsorption capabilities of each sensing material. In this study, changes in the the microcantilever's vibration frequency directly reflects the difference in the adsorption capabilities to NO and NO_2.

Figure 9(a), (b) showed the frequency shift to 100 ppm NO and 10 ppm NO_2 of NiO, respectively. In repeated tests, the frequency shit to NO was greater than that of NO_2, implying NiO preferred to adsorb NO molecules when exposed to NO_x mixture. In a similar manner way, gas adsorption capabilities of $NiFe_2O_4$(+30 wt.% Fe_2O_3) was examined and presented in Figure 10. It is reasonable to concluded that ($NiFe_2O_4$+30 wt.% Fe_2O_3) exhibits similar adsorption capability to both 3 ppm NO_2 and 100 ppm NO, since minor difference in the frequency shit to NO and NO_2 was observed.

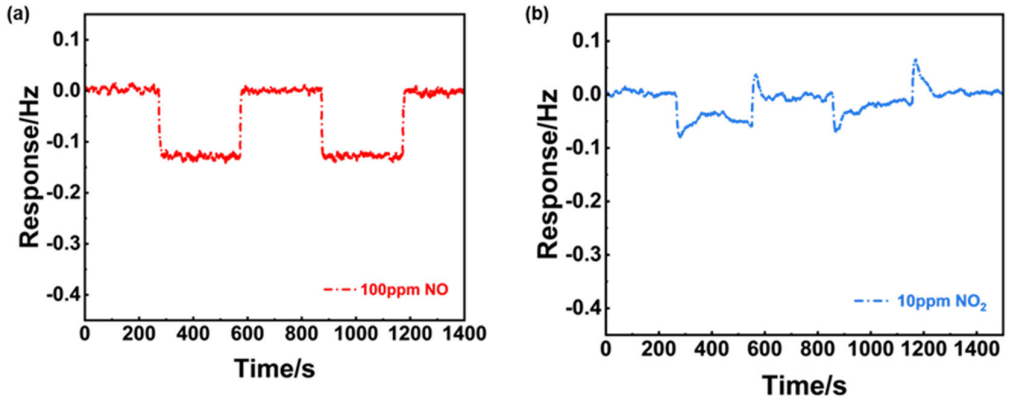

Figure 9. Comparison of the NO and NO_2 gas adsorption for NiO using the resonant microcantilever. (a) response frequency difference of 100 ppm NO; (b) response frequency difference of 10 ppm NO_2.

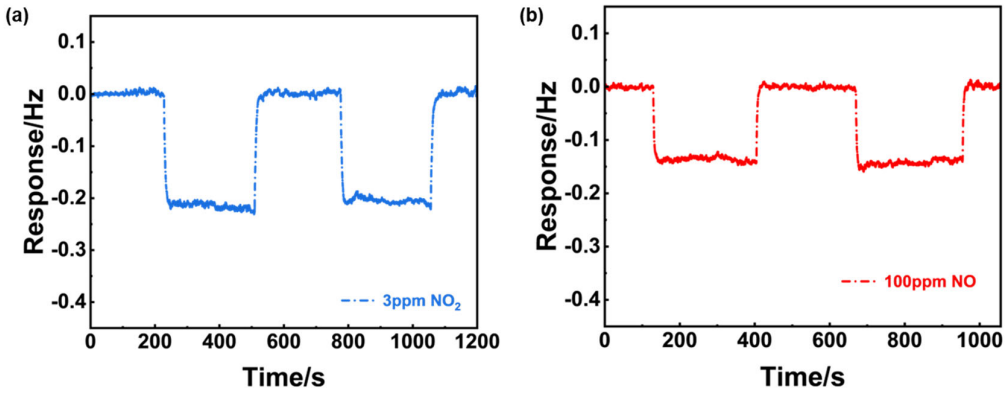

Figure 10. Comparison of the NO and NO_2 gas adsorption for ($NiFe_2O_4$+30 wt.% Fe_2O_3) calcined at 1200°C using the resonant microcantilever. (a) response frequency difference of 3 ppm NO_2; (b) response frequency difference of 100 ppm NO.

To further understand the mechanism for the sensors' different selectivity, polarization curves were measured in the sample gas (3 ppm NO_2, 10 ppm NO_2, 10 ppm NO and 100 ppm NO, in 21% O_2, with N_2 balanced) and air, which could reflect the reaction rate for electrochemical reaction that occurred in TPB (triple phase boundary). Figure 11(a) showed that when the bias voltage was 0 mV, the current value difference between various sample gases at different concentration and air was

 doi:10.20944/preprints202410.1837.v1

small, it can be inferred that NiO-SE had poor electrochemical catalytic activity to NO and NO_2. On the contrary, an obvious current difference between NO_2 and NO was given in Figure 11(b). What's more, a higher current value of NO_2 suggested that the ($NiFe_2O_4$+30 wt.% Fe_2O_3)-SE had better electrochemical catalytic activity of NO_2, compared with NO.

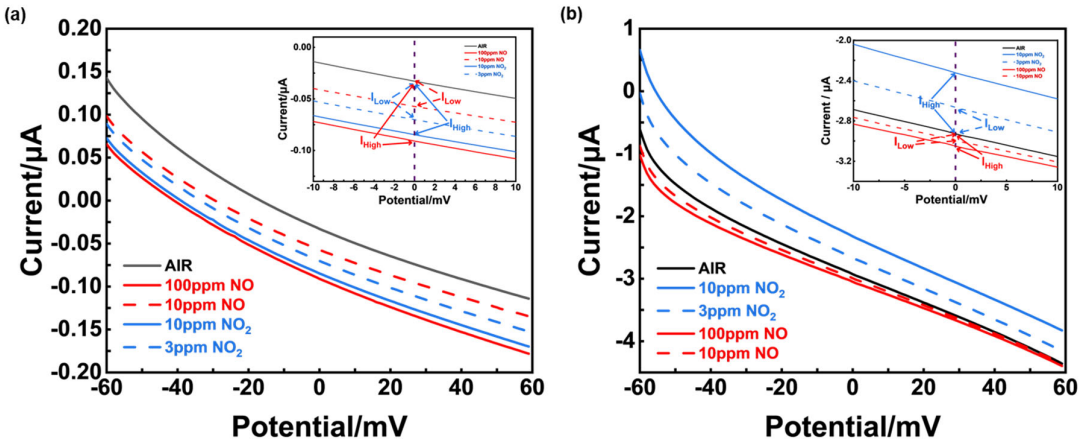

Figure 11. Polarization curves in different concentration of NO and NO_2 using different sensors. (a) Sensor using NiO-SE, operated at 310°C; (b) Sensor using ($NiFe_2O_4$+30 wt.%Fe_2O_3)-SE, operated at 390°C. (I_{High} and I_{Low} represent the current value generated from high concentration or low concentration of NO or NO_2, respectively.).

Through a comparative analysis of gas adsorption capabilities and electrochemical reactivity, we can conclude that the response selectivity of the sensor using NiO-SE primarily arises from its strong adsorption affinity for NO (confirmed by Figure 9). Although NiO exhibits similar electrochemical catalytic activity towards both NO and NO_2 (Figure 11(a)), it demonstrates a significant difference in the adsorption of these gases. Conversely, for the sensor utilizing ($NiFe_2O_4$ + 30 wt.% Fe_2O_3)-SE, the notable selectivity for NO_2 can be attributed to the high electrochemical reactivity of $NiFe_2O_4$ + 30 wt.% Fe_2O_3 with NO_2, as only a minor difference was observed in its adsorption capabilities (as presented in Figure 10 and Figure 11(b)).

4. Conclusions

For the purpose of precisely tracking the level of NOx during iNO treatment, we developed YSZ-based gas sensors comprised of Ni-based SEs and Mn-based RE. These sensors using NiO or ($NiFe_2O_4$+30 wt.% Fe_2O_3)-SE demonstrated high selectivity, desirable stability and excellent repeatability to high level NO or low level NO_2. The working principle of these sensors can be summarized that NO preferred to adsorbed on the surface of NiO while $NiFe_2O_4$+30 wt.% Fe_2O_3 composite demonstrate high electrochemical reactivity to NO_2, resulting in satisfactory sensing characteristics for these sensors in tracking the variation of NO_x. However, it should be noted that due to the high operational temperature of these sensors, it is necessary to overcome the limitations of high power consumption in practical application. In summary, these findings mark a bright future for the application of the robust and high performance NO_x sensors in innovative iNO treatment technologies.

Author Contributions: Conceptualization, Tao Chen, YangBo Zhao, YanYu Zhang and Han Jin; Data curation, ZhengHu Zhang and ChengHan Yi; Formal analysis, ZhengHu Zhang, ChengHan Yi and Han Jin; Investigation, ZhengHu Zhang, ChengHan Yi and Han Jin; Methodology, Han Jin; Project administration, Han Jin; Resources, Tao Chen and Han Jin; Supervision, Han Jin; Validation, ZhengHu Zhang; Visualization, ZhengHu Zhang; Writing – original draft, ZhengHu Zhang; Writing – review & editing, Han Jin.

Data Availability Statement: Correspondence and requests for materials should be addressed to H. Jin.

 doi:10.20944/preprints202410.1837.v1

Acknowledgement: The authors gratefully acknowledge the financial support for this research from the National Natural Science Foundation of China (Grant No. 2022YFE0118800, 62227815, 52000133), "the Belt and Road" young scientist exchange program of the Science and Technology Commission of Shanghai (Grant No. 20490743000), Shanghai Natural Science Foundation (Grant No. WF220403061), Sichuan Natural Science Foundation (Grant No. 2022NSFSC0390, KX002), Oceanic Interdisciplinary Program of Shanghai Jiao Tong University (Grant No. SL2020MS014) and Program of National Key Laboratory (SKLPBS2249).

Conflicts of Interest: The author declare no conflict of interest.

References

1. S.H. Abman, G. Hansmann, S.L. Archer, D.D. Ivy, I. Adatia, W.K. Chung, et al., Pediatric Pulmonary Hypertension, Circulation, 132(2015) 2037-99.
2. A. Keshavarz, H. Kadry, A. Alobaida, F. Ahsan, Newer approaches and novel drugs for inhalational therapy for pulmonary arterial hypertension, Expert Opinion on Drug Delivery, 17(2020) 439-61.
3. J.P. Kinsella, T.A. Parker, D.D. Ivy, S.H. Abman, Noninvasive delivery of inhaled nitric oxide therapy for late pulmonary hypertension in newborn infants with congential diaphragmatic hernia, The Journal of Pediatrics, 142(2003) 397-401.
4. F. Ichinose, J.D. Roberts, W.M. Zapol, Inhaled Nitric Oxide, Circulation, 109(2004) 3106-11.
5. I.R. Preston, K.D. Sagliani, K.E. Roberts, A.M. Shah, S.A. DeSouza, W. Howard, et al., Comparison of Acute Hemodynamic Effects of Inhaled Nitric Oxide and Inhaled Epoprostenol in Patients with Pulmonary Hypertension, Pulmonary Circulation, 3(2013) 68-73.
6. R.J. Barst, R. Channick, D. Ivy, B. Goldstein, Clinical Perspectives with Long-Term Pulsed Inhaled Nitric Oxide for the Treatment of Pulmonary Arterial Hypertension, Pulmonary Circulation, 2(2012) 139-47.
7. M.L. Bernier, L.H. Romer, M.M. Bembea, Spectrum of Current Management of Pediatric Pulmonary Hypertensive Crisis, Critical Care Explorations, 1(2019).
8. R.M. DiBlasi, T.R. Myers, D.R. Hess, Evidence-based clinical practice guideline: inhaled nitric oxide for neonates with acute hypoxic respiratory failure, Respir Care, 55(2010) 1717-45.
9. B. Weinberger, D.L. Laskin, D.E. Heck, J.D. Laskin, The toxicology of inhaled nitric oxide, Toxicol Sci, 59(2001) 5-16.
10. D.M. McMullan, J.M. Bekker, M.J. Johengen, K. Hendricks-Munoz, R. Gerrets, S.M. Black, et al., Inhaled nitric oxide-induced rebound pulmonary hypertension: role for endothelin-1, American Journal of Physiology-Heart and Circulatory Physiology, 280(2001) H777-H85.
11. Y. Liu, Y. Zhu, C. Jiang, Z. Su, Y. Yan, B. Feng, et al., An electrochemical nitric oxide generator for in-home inhalation therapy in pulmonary artery hypertension, BMC Medicine, 20(2022) 481.
12. Q. Li, W. Zeng, Y. Li, Metal oxide gas sensors for detecting NO2 in industrial exhaust gas: Recent developments, Sensors and Actuators B: Chemical, 359(2022).
13. N. Miura, T. Sato, S.A. Anggraini, H. Ikeda, S. Zhuiykov, A review of mixed-potential type zirconia-based gas sensors, Ionics, 20(2014) 901-25.
14. J. Zou, X. Liu, H. Jin, Z. Zhan, J. Jian, NO2 sensing properties of electrode-supported sensor by tape casting and co-firing method, Ionics, 21(2015) 2655-62.
15. J. Fergus, Materials for high temperature electrochemical NOx gas sensors, Sensors and Actuators B: Chemical, 121(2007) 652-63.
16. C.O. Park, N. Miura, Absolute potential analysis of the mixed potential occurring at the oxide/YSZ electrode at high temperature in NO -containing air, Sensors and Actuators B: Chemical, 113(2006) 316-9.
17. K.P. Ramaiyan, R. Mukundan, Editors' Choice—Review—Recent Advances in Mixed Potential Sensors, Journal of The Electrochemical Society, 167(2020) 037547.
18. I. Romanytsia, J.-P. Viricelle, P. Vernoux, C. Pijolat, Application of advanced morphology Au–X (X=YSZ, ZrO2) composites as sensing electrode for solid state mixed-potential exhaust NOx sensor, Sensors and Actuators B: Chemical, 207(2015) 391-7.
19. F. Liu, J. Wang, L. Jiang, R. You, Q. Wang, C. Wang, et al., Compact and planar type rapid response ppb-level SO2 sensor based on stabilized zirconia and SrMoO4 sensing electrode, Sensors and Actuators B: Chemical, 307(2020) 127655.
20. Y. Xu, Z. Liu, J. Lin, J. Zhao, N.D. Hoa, N.V. Hieu, et al., Integrated Smart Gas Tracking Device with Artificially Tailored Selectivity for Real-Time Monitoring Food Freshness, Sensors, 23(2023).
21. S. Lv, Y. Zhang, L. Jiang, L. Zhao, J. Wang, F. Liu, et al., Mixed potential type YSZ-based NO2 sensors with efficient three-dimensional three-phase boundary processed by electrospinning, Sensors and Actuators B: Chemical, 354(2022) 131219.
22. C. Zhang, C. Jiang, X. Zheng, X. Hong, Medium-Low-Temperature NO2 Sensor Based on YSZ Solid Electrolyte and Mesoporous WO3 Sensing Electrode for Detection of Vehicle Emissions, Nano, 16(2021).
23. J. Xu, C. Wang, B. Yang, H. Yu, F. Xia, J. Xiao, Superior sensitive NiFe2O4 electrode for mixed-potential NO2 sensor, Ceramics International, 45(2019) 2962-7.

 doi:10.20944/preprints202410.1837.v1

24. J. Wang, C. Wang, A. Liu, R. You, F. Liu, S. Li, et al., High-response mixed-potential type planar YSZ-based NO2 sensor coupled with CoTiO3 sensing electrode, Sensors and Actuators B: Chemical, 287(2019) 185-90.
25. Y. Chen, Effects of Electrode Microstructures on the Sensitivity and Response Time of Mixed-Potential NO2 Sensor Based on La0.6Sr0.4CoO3 Sensing Electrode, IEEE Sensors Journal, 21(2021) 8621-6.
26. H. Jin, Y. Huang, J. Jian, Plate-like Cr2O3 for highly selective sensing of nitric oxide, Sensors and Actuators B: Chemical, 206(2015) 107-10.
27. H. Jin, Y. Huang, J. Jian, Sensing mechanism of the zirconia-based highly selective NO sensor by using a plate-like Cr2O3 sensing electrode, Sensors and Actuators B: Chemical, 219(2015) 112-8.
28. Y.-L. Liu, H. Wang, Y. Yang, Z.-M. Liu, H.-F. Yang, G.-L. Shen, et al., Hydrogen sulfide sensing properties of NiFe2O4 nanopowder doped with noble metals, Sensors and Actuators B: Chemical, 102(2004) 148-54.
29. S. Zhuiykov, M. Muta, T. Ono, M. Hasei, N. Yamazoe, N. Miura, Stabilized Zirconia-Based NO_x Sensor Using $ZnFe_2O_4$ Sensing Electrode, Electrochemical and Solid-State Letters, 4(2001) H19.
30. H. Liu, J. Wang, H. Yu, H. Xiong, Y. Chen, C. Wang, et al., Promoted Carbon Monoxide Sensing Performance of a Bi2Mn4O10-Based Mixed-Potential Sensor by Regulating Oxygen Vacancies, ACS Sensors, 7(2022) 2978-86.
31. C. Zheng, Y. Shi, B. Tang, J. Zhang, Black Phosphorus–Tungsten Oxide Sandwich-like Nanostructures for Highly Selective NO2 Detection, Sensors2024.
32. (!!! INVALID CITATION !!! [33, 34]).
33. K.M. Goeders, J.S. Colton, L.A. Bottomley, Microcantilevers: Sensing Chemical Interactions via Mechanical Motion, Chemical Reviews, 108(2008) 522-42.
34. T. Xu, P. Xu, D. Zheng, H. Yu, X. Li, Metal–Organic Frameworks for Resonant-Gravimetric Detection of Trace-Level Xylene Molecules, Analytical Chemistry, 88(2016) 12234-40.